Aeroelastic Coupling between a Thin Divergent and High Pressure Jets

Eric Schall* — Raphael Lardat** — Alain Dervieux**
Bruno Koobus*** — Charbel Farhat****

*Université de Pau, IUT Génie Thermique et Energétique, 1, Avenue de l'Université,
F-64000 PAU, Eric.Schall@univ-pau.fr
** INRIA, 2003 Route des Lucioles, F-06902 Sophia-Antipolis Cedex,
Raphael.Lardat@Inria.fr, Alain.Dervieux@Inria.fr
*** Université de Montpellier II, Place Eugène Bataillon, Département de
Mathématiques, CC 051, F-34095 Montpellier Cedex 5 and INRIA,
****University of Colorado at Boulder, Campus Box 429, Dept. of Aerospace Eng.
Sciences, Boulder, Colorado 80309-0429, U.S.A, charbel@boulder.colorado.edu

ABSTRACT. Rocket divergents concentrate the engine thrust on a light structure. This thrust may provoke deformations, and these deformations may influence the jet. For analysis, we formulate a coupled fluid/structure/moving grid problem, which leads to a numerical model involving a three-field Arbitrary Lagrangian- Eulerian method offering second-order spatial accuracy. It employs a time-staggered procedure for global second-order accurate time-integration of the corresponding coupled semi-discrete equations. We present the transient aeroelastic response obtained with a simplified geometry of divergent when the flow condition induces shock waves either behind or inside the nozzle, for structural designs of small stiffness.

RÉSUMÉ. Dans les divergents de fusée, la poussée est concentrée sur une structure légère. Cette poussée peut provoquer des déformations qui peuvent influencer l'écoulement du jet. Pour analyser ce phénomène, on résout un problème à trois champs : fluide/structure/grille déformable, en utilisant une formulation d'Euler-Lagrange-Arbitraire. La méthodologie numérique développée est précise au second ordre en espace. Concernant le couplage temporel des équations semidiscrétisées, une procédure décalée est utilisée, assurant une précision globale du second ordre en temps. On présente la réponse aéroélastique obtenue avec une géométrie simplifiée de divergent pour des configurations d'écoulement impliquant un choc, soit a l'intérieur, soit en sortie du divergent.

KEYWORDS: fluid/structure interaction, Arbitrary-Lagrangian-Eulerian formulation, divergent, supersonic jet, Euler equations.

MOTS-CLÉS : interaction fluide/structure, formulation d'Euler-Lagrange-Arbitraire, divergent, jet supersonique, équations d'Euler.

1. Introduction

Any one who has examined the movie of the starting of a rocket could note how violent is the transient interaction of hot gases rushing out from the engine divergent. These jets are of high pressure and therefore fastly accelerate to a high supersonic regime before reaching the end of the divergent. Loads induced by supersonic flows on aerodynamical surfaces can lead to transient effects with sometimes flutter phenomena. A well known example is the flutter of a flat panel when a fast enough supersonic flow is applied along it [ASH 62]. The panel instability problem can be already simulated by 2D calculations relying on a classical Euler model for the fluid flow.

Some papers also show this kind of behavior for axisymmetric nozzles under the action of an axisymmetric flow [LEF 00], [LDV 00]. In that case, the excited mode is not one of the main modes of the nozzle structure. Indeed, for generic divergents the first main modes are not axisymmetric. The purpose of the present work is to consider non-axisymmetrical coupling between an inviscid flow and a simplified model of divergent (or nozzle). Different flow configurations involving shock waves behind or inside the nozzle are considered, and the possibly flutter phenomenon is investigated in each case. For investigating the instability nozzle problem, the software developed at University of Colorado (Boulder) in cooperation with INRIA is used.

The rest of this paper is organized as follows: in Section 2, we present the formulation of transient non-linear aeroelastic problems. In Section 3, we summarize the numerical methodology for solving the non-linear aeroelastic problem of the nozzle, and especially the space- and time-discretization, and the partitioned solution procedure. In Section 4, we present the instability nozzle problem. We describe the structure and flow problems, the structural eigen modes, and the transient aeroelastic simulations. Then we comment on the results obtained. Finally, in Section 5 we conclude th is paper.

2. Formulation of transient nonlinear aeroelastic problems

The problem of the motion of the fluid/structure interface that occurs in coupled aeroelastic problems is addressed by solving the fluid equations on deformable dynamic meshes. An Arbitrary Lagrangian Eulerian (ALE) [DON 82],[FLM 95] formulation is used in order to perform the integration of the fluid equations on a moving mesh. The coupled aeroelastic problem to be solved can then be viewed as a three-field problem [FAR 95],[FLM 95]: the fluid, the structure and the dynamic mesh which is

represented by a pseudo-structural system. The semi-discrete equations governing the three-way coupled problem can be written as follows:

$$
\begin{aligned}
\frac{\partial}{\partial t}(V(x,t)w(t)) + F^c(w(t),x,\dot{x}) &= R(w(t),x) \\
M\frac{\partial^2 q}{\partial t^2} + f^{int}(q) &= f^{ext}(w(t),x) \\
\tilde{M}\frac{\partial^2 x}{\partial t^2} + \tilde{D}\frac{\partial x}{\partial t} + \tilde{K}x &= K_c q
\end{aligned}
\qquad [1]
$$

where t designates time, x the position of a moving fluid grid point, w is the fluid state vector, V results from the finite element/volume discretization of the fluid equations, F^c is the vector of convective ALE fluxes, R is the vector of diffusive fluxes, q is the structural displacement vector, f^{int} denotes the vector of internal forces in the structure, f^{ext} the vector of external forces, M is the finite element mass matrix of the structure, $\tilde{M}$, $\tilde{D}$ and $\tilde{K}$ are fictitious mass, damping and stiffness matrices associated with the moving fluid grid and K_c is a transfer matrix that describes the action of the motion of the structural side of the fluid/structure interface on the fluid dynamic mesh.

3. Numerical methodology for solving coupled non-linear aeroelastic problems

In this section, we give the main features of the numerical methods employed in this work for solving the coupled non-linear aeroelastic problem given by Eqs.[1] . For more details, the reader is invited to examine the references given in the text.

3.1. *Discretization of transient non-linear aeroelastic problems*

Spatial discretization

The spatial discretization of the fluid equations is based on a finite element/finite volume formulation on unstructured meshes. It combines a Roe upwind scheme for computing the convective fluxes, and a Galerkin centered method for evaluating the viscous terms. Second-order space accuracy is achieved through a piecewise linear interpolation method based on the MUSCL (Monotonic Upwind Scheme for Conservation Laws) procedure [VAN 79],[DER 85], and a slope limitation algorithm [ALB 82] can be employed in order to damp or eliminate the spurious oscillations that may occur in the vicinity of discontinuities. For addressing the problem of flow simulations on moving grids, an ALE formulation is incorporated in the flow solver. The numerical algorithms used with this ALE formulation satisfy the Geometric Conservation Laws (GCL) [LES 95],[NKO 94] that govern flow computations on moving grids.

The structure is represented by a finite element model, and its dynamics behavior is predicted using the true displacement, velocity and acceleration degrees of freedom.

At selective time-steps of an aeroelastic simulation, the dynamic fluid mesh is updated to conform the most recently computed configuration of the structure. The

points lying on the fluid/structure boundary are first adjusted to conform to the new position of the surface of the structure, then the remainder of the fluid grid points are repositioned accordingly. In the methodology used in this work, the new position of the interior grid points is determined from the displacement solution of a discrete pseudo-structural problem representing the unstructured dynamic fluid mesh. The pseudo-structural system is constructed by lumping a fictitious mass at each vertex of the fluid mesh and attaching fictitious lineal springs to each edge connecting two vertices [BAT 89],[FLM 95],[FAR 95]. This discrete system is represented by the third of Eqs. (1) where $\tilde{M} = \tilde{D} = 0$.

Finally, in fluid/structure interaction problems the fluid and structure meshes have often non-matching discrete interfaces. In that case, we use the load and motion transfer algorithms described in [FAR 00] for evaluating properly the pressure forces on the surface of the structure, and transferring correctly the structural motion to the fluid mesh. In particular, the loads induced by the fluid on the structure are computed in a conservative way.

Time discretization

For solving accurately and efficiently the flow equations given by the first of Eqs.[1] on dynamic meshes, a second-order time-accurate implicit algorithm preserving the GCL [KOO 99] is employed. The time discretization is based on a second-order backward difference scheme. The non-linear flow equations derived from the time-discretization are solved by a defect-correction (Newton-like) method [BOH 84], [MAR 96].

The structural equations of dynamic equilibrium given by the second of Eqs. (1) are solved with a second-order time-accurate implicit scheme where the trapezoidal method is used.

3.2. *Staggered solution procedure*

The solution of the coupled fluid/structure problem [1] is computed by a staggered solution procedure in the time domain [FLM 95],[FAR 97]. More precisely, we use the staggered algorithm given in [FAR 96] which satisfies the GCL as well as the continuity of both the displacement and velocity fields at the fluid/structure interface. This algorithm can be written as follows:

1. Using the mesh position $x^{n-\frac{1}{2}}$, and the mesh velocity $\dot{x}^n$ that matches the structural velocity $\dot{q}^n$ on the fluid/structure interface, update the mesh coordinates as follows:

$$x^{n+\frac{1}{2}} = x^{n-\frac{1}{2}} + \Delta t \dot{x}^n$$

2. Using $x^{n-\frac{1}{2}}$, $x^{n+\frac{1}{2}}$ and $\dot{x}^n$, update the fluid state vector $w^{n+\frac{1}{2}}$ in a manner that satisfies the GCL;

3. Using the pressure computed from $w^{n+\frac{1}{2}}$, compute q^{n+1} and $\dot{q}^{n+1}$ using the midpoint rule.

4. Aeroelastic coupling between a nozzle and a supersonic jet

4.1. *Description of the structure and flow problems*

In this paper, we consider a simple structural model of a nozzle made with a cone-shaped part, a divergent, and a stiffener at the exit. The nozzle discretized in 9300 nodes is represented by an equivalent finite element model with 18400 triangular shell elements for the cone-shaped part and the divergent, and 100 beam elements for the stiffener (Fig. 1). The nozzle is clamped at its base, and immersed in the flow domain which is discretized into 87648 vertices and 483912 unstructured tetrahedra. A partial view of the fluid mesh is shown in Fig. 2.

The fluid mesh is decomposed into 14 subdomains and assigned to 14 processors for parallel computations. The finite element structural model is sequentially computed and therefore is not partitioned.

In this work, two different flow configurations are considered: depending on the inflow pressure, shock waves occur behind or inside the nozzle. For both configurations, the inflow density and Mach number are respectively set to $\rho_{inflow} = 0.423 \ kg/m^3$ and $M_{inflow} = 1$, and the outflow condition corresponds to the ambiant air. The value of the inflow pressure is taken either to $P_{inflow} = 1060000 \ Pa$ (shock wave behind the nozzle) or $P_{inflow} = 230000 \ Pa$ (shock wave inside the nozzle).
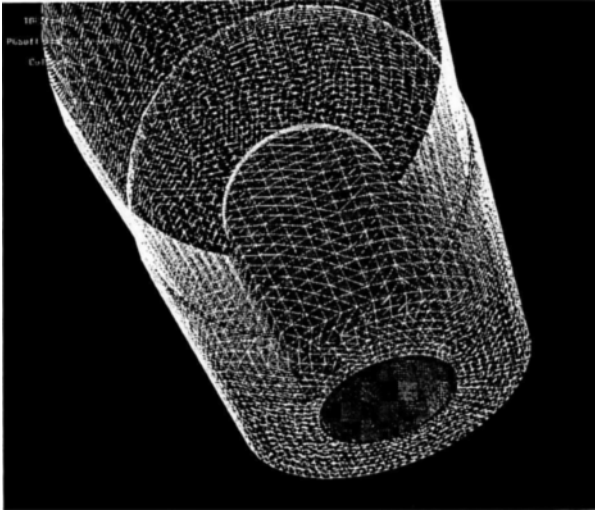

Figure 1. *Finite element model of the nozzle*

Figure 2. *Partial view of the fluid mesh of the nozzle and the immersed structure mesh.*

4.2. *Transient aeroelastic simulations*

The first fundamental modes of the structure are computed, and as expected, they are not axisymmetric. This tends to prove that a truly three-dimensional aeroelastic computation is necessary for simulating realistic nozzle coupled problems which are dominated by the first fundamental modes. The first structural mode corresponds to an ovalization mode whose frequency is $freq = 25\ Hz$ (Fig. 3).

In a first step, the finite element structural model of the nozzle is perturbed along its first fundamental mode, and a steady state solution is computed around the deformed shape of the nozzle.

For an inflow pressure value $P_{inflow} = 1060000\ Pa$, external Mach stems are obtained as depicted in Fig. 4. One can notice a large fluid acceleration inside the nozzle and oblique shock waves attached to the exit. In the jet downstream nozzle, there is a barrell-like structure, as well as a slip discontinuity at the boundary of this jet.

For an inflow pressure value $P_{inflow} = 230000\ Pa$, one can remark the presence of a normal shock wave preceding a subsonic zone inside the nozzle (see Fig. 5). Next, this perturbation is used as an initial condition, and the aeroelastic response of the nozzle is computed by the partitioned procedure described in the previous section. The objective is to predict numerically the subsequent nozzle motion and flow evolution for both flow conditions.

For this dynamics problem, the time-step of the structure problem is set to
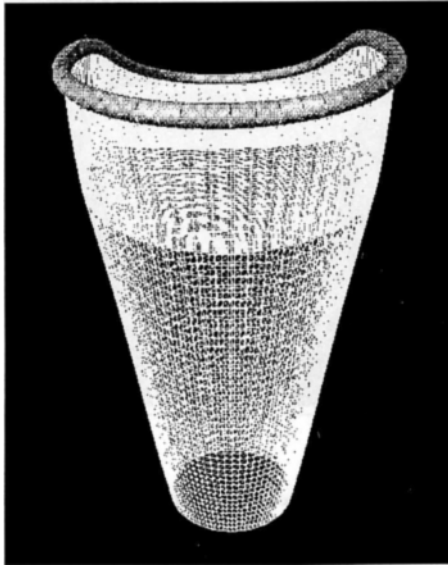
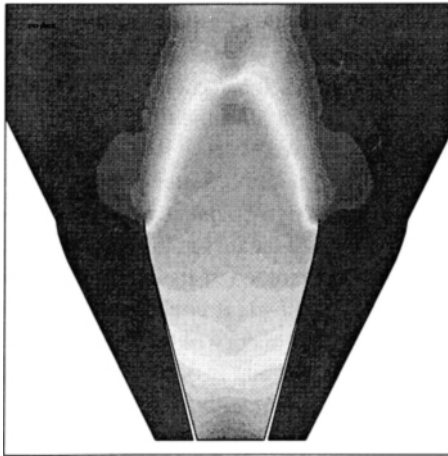**Figure 3.** *First fundamental mode. The enlarged shape at the exit of the nozzle corresponds with the stiffener*

Figure 4. *Zoom of the Mach isovalues in the nozzle region for an inflow pressure set to* 1060000 *Pa*
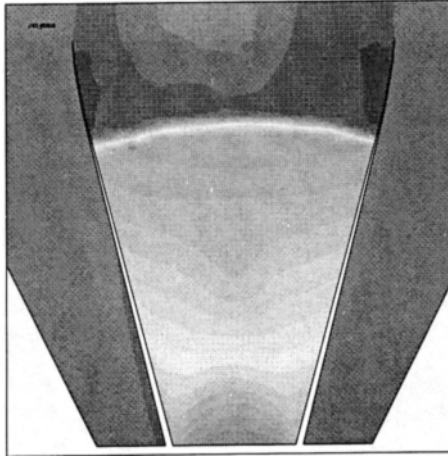
Figure 5. *Zoom of the Mach isovalues in the nozzle region for an inflow pressure set to* $230000\ Pa$

$\Delta t_S = T_6/80 = 0.00025\ s.$, where T_6 denotes the period of the sixth mode of the nozzle. For the flow solver, the CFL number is set to 100. It turns out that for the given fluid mesh, this value of the CFL number corresponds to an average value of the fluid time-step over the duration of the aeroelastic simulation $\Delta t_F = \Delta t_S$. The aeroelastic response obtained for both case of flow configurations is described hereafter.

   $- P_{inflow} = 1060000\ Pa$. With this flow condition, we have a large fluid acceleration inside the nozzle and oblique shock waves attached to the exit. The obtained radial displacement history of points located on the stiffener (point $p1$) and on the nozzle wall at 25% of the total length after the throat (point $p2$) is depicted in Fig. 6 for the first 0.2 physical seconds. We observe that the motion of the nozzle around its initial configuration is damped, and no flutter phenomenon accurs with this flow condition. The presence of small high frequency perturbations on the displacement history corresponding with the point located at 25% of the nozzle length is probably due to the fact that the nozzle is clamped at its base and its stiffness. Fig. 7 shows the evolution of the pressure at point $p1$, it consists in a damped oscillating average signal with small perturbations. The history of the longitudinal resulting force due to the pressure acting on the nozzle surface is depicted in Fig. 8. We remark that the averaged signal of this force is constant with time, and that the amplitude of the high frequency component of this signal is less than one percent of the averaged force.

   $- P_{inflow} = 230000\ Pa$. With this flow condition, we have a normal shock wave inside the nozzle. Because of the nozzle geometry and the simulation of an Euler flow, the shock wave induces no flow separation. The obtained displacement history of points located on the stiffener (point $p1$) and on the nozzle at 25% of the total length after the throat (point $p2$) is depicted in Fig.9. As previously, the initial
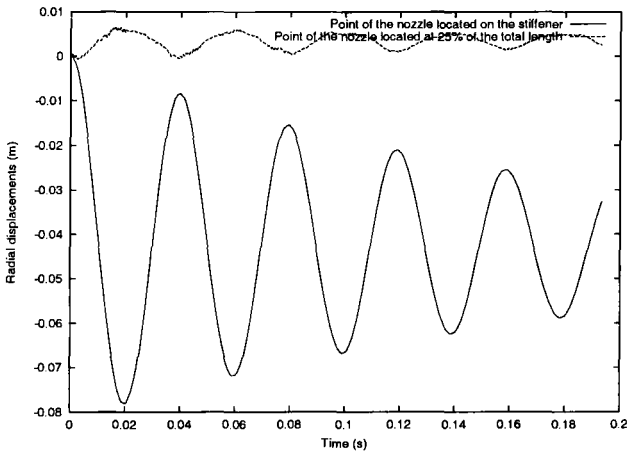
Figure 6. *Radial displacement history for an inflow pressure set to* 1060000 *Pa*
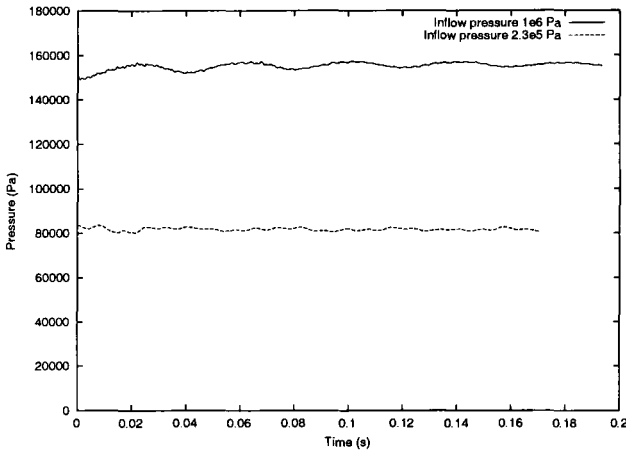

Figure 7. *Pressure history at point* p1

perturbation is damped, and no flutter phenomenon occurs. The pressure history at point p1 and the history of the longitudinal resulting force due to the pressure acting on the nozzle surface are respectively depicted in Fig.7 and Fig. 8.The remarks made for the previous flow conditions are still valid.

Both aeroelastic problems have required around 800 coupled time-steps for the first 0.2 second of the transient aeroelastic response of the nozzle, and a total simulation time evaluated to 4 hours on a 15-processor SGI Origin 2000 machine.
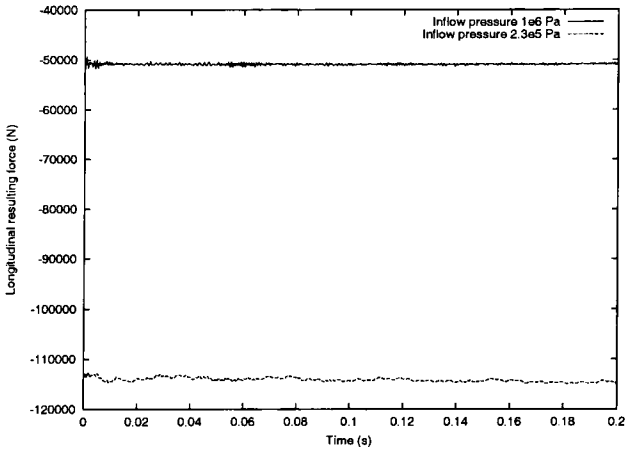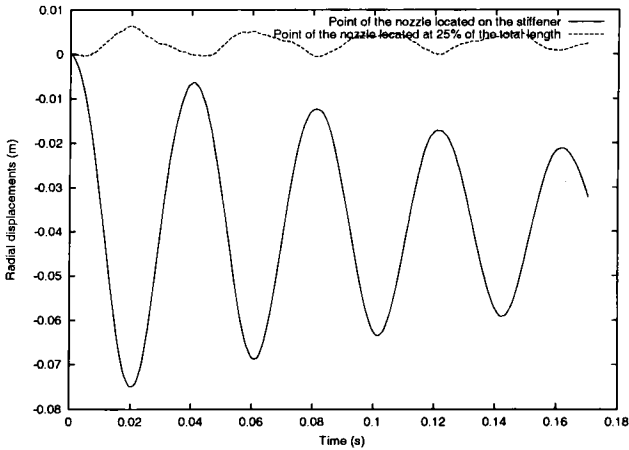
Figure 8. *Longitudinal resulting force history*

Figure 9. *Radial displacement history for an inflow pressure set to* 230000 Pa

5. Structure stiffness influence

We now investigate the influence of the stiffness of the different components of the structure (shell and stiffener); more precisely we shall compare the behavior of three structures:

– a first one, **(S1)**, has a rather rigid shell (cone+divergent), and a strong stiffener; we shall call it the reference structure;

– in a second one, **(S2)**, the shell is weakened by a two times thinner shell, the stiffener is unchanged;

– in a third one, **(S3)**, the shell is same as in reference, but the stiffener is weakened by a factor 100 (applied to the cross section).

Besides these structural options, we shall consider the two above "flow conditions":

– **(P1)** is the high pressure flow with oblique shock depicted in Fig.4,

– **(P2)** is the lower pressure flow with normal shock depicted in Fig.5.

It is first interesting to evaluate the global reaction (amplification, damping) of the different structures for the two flow conditions. In all calculation, the initial position of shell is a deformation by the first (bilobate) eigenmode, as in Fig.10.

In Fig.11, the oblique-shock **(P1)** flow is tested with the structures (S1) and (S3). It is predicible that the oscillation frequency will be lower with a weaker stiffener, but we also assess that the stiffener is necessary for mastering the arising of high frequencies (about 20 times larger). We present in (Figs. 12 to 15) some snapshot of
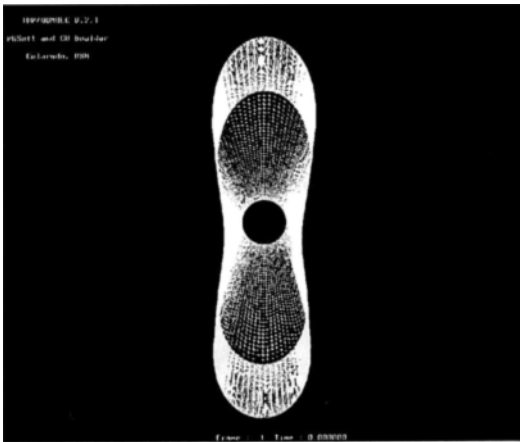

Figure 10. *Initial shell shape for all calculations, i.e. first mode (artificial amplification by a factor 16)*

the calculation with weak stiffener; we observe that the bilobate oscillation is more or less well conserved, but with higher frequency interacting. These high frequencies are visible at two levels, i.e. at the level of the lip plane (already just after the starting of simulation (Fig.12)) and also transversely (Fig. 15).   We then compute the second flow context,**(P2)**, with a lower pressure and a normal shock inside the divergent. We have computed the three structure configurations. In Fig.16 we observe that the stiffener has a predominant role since the structure movement is well changed when the stiffener is weak. We concentrate on this last combination, P2 flow and S3 structure: the reason of change in amplitude and frequency is easily explained by the changing in oscillation mode, that is produced at early starting, since from the fundamental bilobate mode, a trilobate mode appears in the first oscillation, Figs.10, 17, 18.
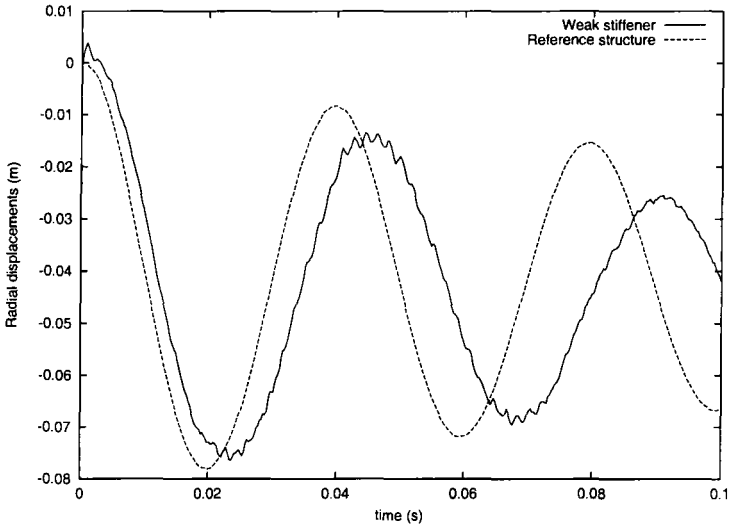
Figure 11. *Behavior with a weaker stiffener and oblique shock: comparison of shell motion with reference structure and thinner one*
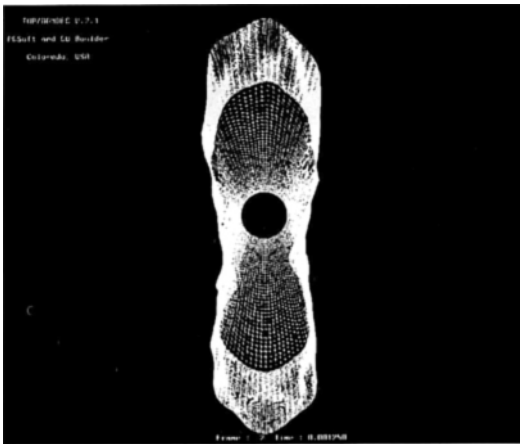

Figure 12. *Behavior with a weaker stiffener and oblique shock : shell shape after a tenth period (artificial amplification by a factor 16)*
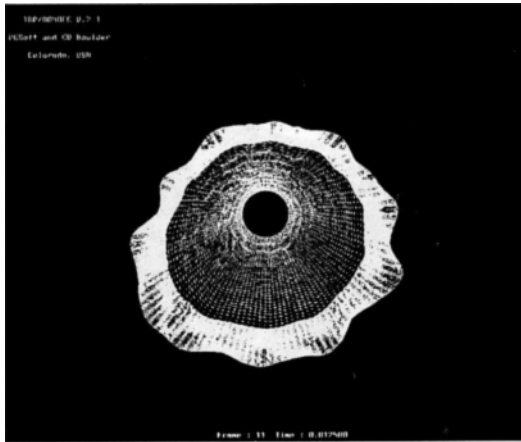
Figure 13. *Behavior with a weaker stiffener and oblique shock: shell shape after half a period (artificial amplification by a factor 16)*
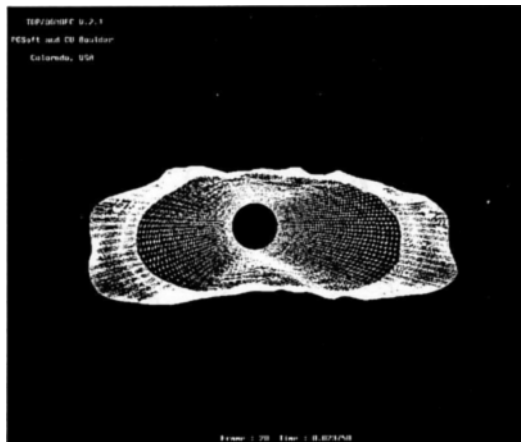

Figure 14. *Behavior with a weaker stiffener and oblique shock: shell shape after a complete period (artificial amplification by a factor 16)*
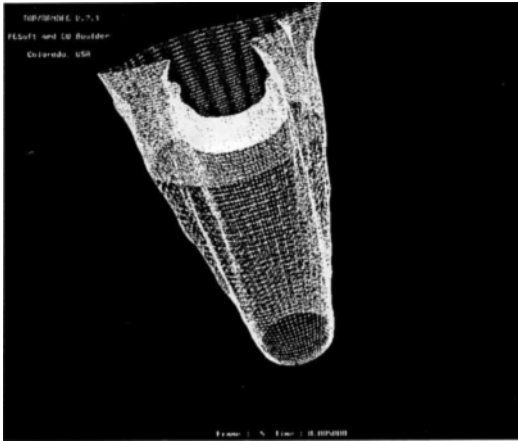
Figure 15. *Behavior with a weaker stiffener and oblique shock: shell shape after a tenth period (artificial amplification by a factor 16)*
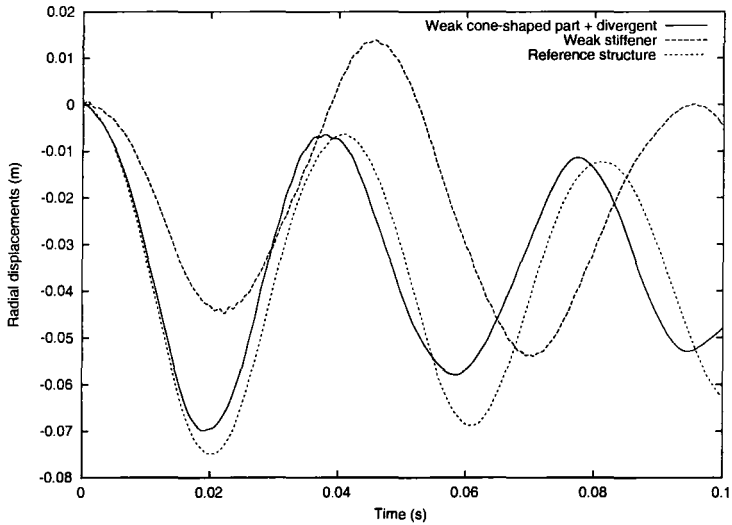

Figure 16. *Behavior with a weaker stiffener and normal shock: comparison of shell motion with reference structure and thinner one*

Figure 17. *Behavior with a weaker stiffener and normal shock inside divergent: shell shape after half a period, the number of lobes is unclear (artificial amplification by a factor 16)*

Figure 18. *Behavior with a weaker stiffener and normal shock : shell shape just after a complete period : (artificial amplification by a factor 16)*

6. Conclusion

In this paper, we have addressed the problem of simulating aeroelastic coupling between a nozzle and a supersonic jet. More specifically, no axisymmetric assumptions have been done, and we have considered truly three-dimensional jet/nozzle coupled problems with different flow conditions involving shocks either downstream or inside the nozzle. In this work, the flow has been assumed non viscous. We have observed that, for the investigated flow conditions, and with the given geometry and material features of the nozzle, an initial perturbation is damped with time and no flutter phenomenon occurs.

A hightly supersonic flow excitates high frequencies while keeping the main bilobate mode. A less fast supersonic flow with normal shock inside the divergent provokes changes in the shape of oscillation mode. The important role of the stiffener is also stressed. This study will contribute to the *a priori* specification of a series of experiments. It will be pursued by applying the turbulence modelling capacities of the AERO software.

Acknowledgements

7. References

[ASH 62] BISPLINGHOFF R.L. AND ASHLEY H., "Principle of Aeroelasticity", *Dover Publications*, In., 1962.

[LEF 00] LEFRANCOIS E., DHATT G. AND VANDROMME D., "Fluid-Structural Interactions with Apllications to Rocket Engines", *Internat. J. Numer. Meths. Fluids*, in press.

[LDV 00] LEFRANCOIS E., DHATT G. AND VANDROMME D., *this issue*.

[DON 82] DONEA J., "An Arbitrary Lagrangian-Eulerian Finite Element Method for Transient Fluid-Structure Interactions", *Comput. Meths. Appl. Mech. Engrg.* 1982, 33, p. 689-723

[FLM 95] FARHAT C., LESOINNE M. AND MAMAN N., "Mixed Explicit/Implicit Time Integration of Coupled Aeroelastic Problems: Three-Field Formulation, Geometric Conservation and Distributed Solution", *Internat. J. Numer. Meths. Fluids* 21 (1995), p. 807-835

[FAR 95] FARHAT C., "High Performance Simulation of Coupled non-linear Transient Aeroelastic Problems", *AGARD Report* R-807, Special Course on Parallel Computing in CFD (l'A rodynamique numérique et le calcul en parallèle, North Atlantic Treaty Organization (NATO), October 1995.

[VAN 79] VAN LEER B., "Towards the Ultimate Conservative Difference Scheme V: a Second-Order Sequel to Godunov's Method", *J. Comp. Phys.* 1979, 32, p. 361-370

[DER 85] DERVIEUX A., "Steady Euler Simulations Using Unstructured Meshes", *Von Karman Institute Lecture Series*, 1985.

[ALB 82] VAN ALBADA G.D., VAN LEER B. AND ROBERTS W. W., "A Comparative Study of Computational Methods in Cosmic Gas Dynamics", *Astron. Astrophys.* 1982, 108, p. 76-84

[LES 95] LESOINNE M. AND FARHAT C., "Geometric Conservation Laws for Aeroelastic Computations Using Unstructured Dynamic Meshes", *AIAA Paper* 95-1709, 12th AIAA Computational Fluid Dynamics Conference, June 19-22, 1995, San Diego, CA.

[NKO 94] NKONGA B. AND GUILLARD H., "Godunov Type Methods on Non-Structured Meshes for Three-Dimensional Moving Boundary Problems", *Comp. Methods Appl. Mech. Engrg.* 113 (1994) p. 183-204

[KOO 99] KOOBUS B. AND FARHAT C., "Second-Order Time-Accurate and Geometrically Conservative Implicit Schemes for Flow Computations on Unstructured Dynamic Meshes", *Computer Methods in Applied Mechanics and Engineering*, Vol. 170, p. 103-130 (1999).

[BAT 89] BATINA J.T., "Unsteady Euler Airfoil Solutions Using Unstructured Dynamic Meshes", *AIAA paper* 89-0115, AIAA 27th Aerospace Sciences Meeting, Reno, Nevada, January 9-12, 1989.

[FAR 00] FARHAT C., LESOINNE M. AND LE TALLEC P., "Load and Motion Transfer Algorithms for Fluid/Structure Interaction Problems with Non-Matching Discrete Interfaces: Momentum and Energy Conservation, Optimal Discretization and Application to Aeroelasticity", *Computer Methods in Applied Mechanics and Engineering*, Vol. 157, p. 95-114, 1998.

[BOH 84] BOHMER K., HEMKER P., AND STETTER H., "The Defect Correction Approach", *Comput. Supp.* 1984, 5:1-32.

[MAR 96] MARTIN R. AND GUILLARD H., "A Second-Order Defect Correction Scheme for Unsteady Problems", *Comput. and Fluids* 1996, 25, p.9-27

[FAR 97] FARHAT C., LESOINNE M., STERN P. AND LANTERI S., "High Performance Solution Procedure of Three-Dimensional Non-Linear Aeroelastic Problems via Parallel Partitioned Algorithms: Methodology and Preliminary Results", *Advances in Engineering Software*,1997, 28, p. 43-61

[FAR 96] FARHAT C. AND LESOINNE M., "On the Accuracy, Stability and Performance of the Solution of Three-Dimensional Non-Linear Transient Aeroelastic Problems by Partitioned Procedures", *AIAA Paper* 96-1388, 37th AIAA/ASME/ASCE/AHS /ASC Structures, Structural Dynamics and Materials Conference, April 18-19, 1996, Salt Lake City, UT.